KU LEUVEN

WP EN2014-12

DC power flow in unit commitment models

Kenneth Van den Bergh, Erik Delarue and William D'haeseleer

TME Working Paper - Energy and Environment
Last update: May 2014

KU Leuven Energy Institute
TME Branch

Contents

Chapter 1

Introduction

Unit commitment models determine the optimal scheduling of a given set of power plants in order to meet the electricity demand. Unit commitment models are purely operational models, minimizing the total system costs (e.g., fuel costs, CO_2 emission costs, start-up costs). The cost minimization is subject to the market clearing condition (i.e., supply equals demand) and technical power plant constraints (e.g., generation limits, minimum up and down times, ramping limits).

Unit commitment models are generation scheduling models, determining the power output of each power plant. However, electricity grids might constrain the scheduling of power plants. The generation scheduling is subject to limited transmission capacity between the different generating units and loads. The power flows through the grid are determined by the physical laws of electricity. Therefore, it is essential to include - at least to a certain extent - grid constraints in unit commitment models. A unit commitment model which takes into account network characteristics and constraints is referred to as a security constrained unit commitment model (SCUC).

Several grid representations exist, with a different accuracy and computational complexity. A commonly used network model is the AC power flow, but due to its computational complexity, it is very little used in unit commitment models. An often used network model in unit commitment models is the DC power flow. The DC power flow is a linearization of the AC power flow and combines computational simplicity - since it is a set of linear equations - with an acceptable level of accuracy.

This text gives a comprehensive overview of grid modeling in unit commitment models, with particular focus on the DC power flow representation. The text presents a detailed description of the DC power flow formulation, as it can be used in unit commitment models.

Chapter 2 starts with a description of an AC electricity grid. In section 3, the basic DC power flow is discussed in detail. Section 4 zooms in on the modeling of power flow controlling devices in DC power flow, i.e., phase shifting transformers and high voltage DC lines. In section 5, the differences between nodal and zonal grid models are discussed. Section 6 deals with N-1 security. Section 7 describes the implementation of the DC power flow in unit commitment models. Section 8 concludes. The appendices to this text discuss the AC power flow and transmission losses. Throughout the chapter, all concepts are applied to a simple network.

Chapter 2

Description of an AC grid

This section presents a description of an AC electricity grid to start with. The notation[1] and sign convention in this section are taken from Elgerd [1]. Other books on power systems might use a different notation or sign convention.

Consider the simple electricity system of figure 2.1. The system consists of 5 nodes or buses (1, 2, 3, 4, 5) and 6 transmission lines (12, 13, 24, 34, 35, 45). N represents the set of nodes and L the set of transmission lines. Each node can be connected to a set of generators and/or a set of loads. The flow through a line is positive if flowing from the node corresponding to the first indices to the node corresponding to the second indices. This network is used as running example throughout the text.

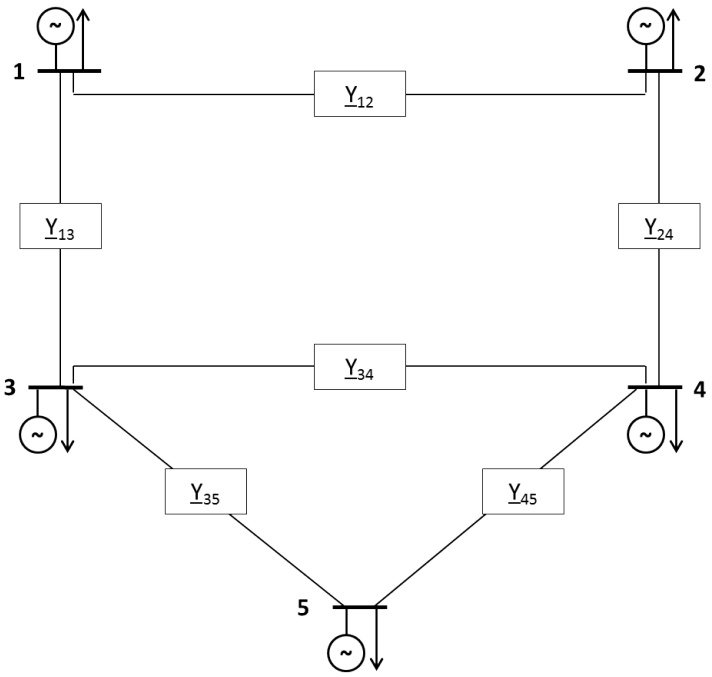

Figure 2.1: Electricity grid with 5 nodes and 6 transmission lines. Each node is connected to a generation unit and a load. This network is used as running example throughout the text.

[1]Parameters in bold and uppercase are matrices (e.g., **PTDF**). Parameters in bold and lowercase are vectors (e.g., $\mathbf{p}_L$). Underlined parameters are complex numbers (e.g., $\underline{Z}$).

Each node is characterized by the following node parameters:

- $\underline{I}_N$: injected current at node N in [A]. A positive current corresponds to a current injection in the grid and vice versa.
- $\underline{V}_N$: voltage at node N in [V]. Another way to write the voltage is $\underline{V}_N = |V_N| \cdot e^{j\,\delta_N}$ with δ_N the voltage angle at node N in [radians], relative to a reference node with zero reference angle.
- P_N: active power injection in the grid at node N in [W]. If nodal generation exceeds nodal load, the net active power is positive and active power is injected in the grid. If nodal load exceeds nodal generation, the net active power is negative and active power is taken from the grid.
- Q_N: reactive power injection in the grid at node N in [VAr]. Net reactive power injection is positive for capacitive nodes and negative for inductive nodes.
- $\underline{S}_N$: total power injection at node N in [VA]. Positive power injections correspond to power injection in the grid, negative power injections correspond power off-takes. The magnitude of $\underline{S}_N$ is referred to as the apparent power. The total power injection is linked to the previous node parameters as follows:

$$\underline{S}_N = \underline{V}_N \cdot \underline{I}_N^* = P_N + j \cdot Q_N \tag{2.1}$$

Each transmission line can be described, in its most simplified form, by a series RL branch[2], a current flow and a voltage drop:

- R_L: resistance of transmission line L in [Ω].
- X_L: reactance of transmission line L in [Ω].
- $\underline{Z}_L$: impedance of transmission line L in [Ω]. The impedance is linked to the resistance and reactance as follows:

$$\underline{Z}_L = R_L + j \cdot X_L \tag{2.2}$$

- $\underline{I}_L$: current through transmission line L in [A]. The positive direction of each line current can be chosen by sign convention.
- $\underline{V}_L$: voltage drop over transmission line L in [V].

Sometimes, the inverse line parameters are used:

- G_L: conductance of transmission line L in [S].
- B_L: susceptance of transmission line L in [S].
- $\underline{Y}_L$: admittance of transmission line L in [S]. The admittance is linked to the previous line parameters as follows:

$$\underline{Y}_L = G_L + j \cdot B_L = \frac{1}{\underline{Z}_L} = \frac{R_L}{{R_L}^2 + {X_L}^2} - j\frac{X_L}{{R_L}^2 + {X_L}^2} \tag{2.3}$$

[2] A line shorter than 500 km can be represented by lumped parameters, instead of distributed parameters. For a line shorter than 100 km, the shunt capacitance and the shunt susceptance can be neglected.

The network is described by its incidence matrix **A** and its bus admittance matrix **Y**. The incidence matrix is a L×N-matrix describing the topology of the network (i.e., which lines are connected to which nodes). The incidence matrix relates the node parameters $\underline{\mathrm{I}}_N$ and $\underline{\mathrm{V}}_N$ with the line parameters $\underline{\mathrm{I}}_L$ and $\underline{\mathrm{V}}_L$. The admittance matrix is a N×N-matrix, relating the nodal voltages $\underline{\mathrm{V}}_N$ with the injected nodal currents $\underline{\mathrm{I}}_N$. Knowledge of the incidence matrix is necessary to determine the admittance matrix. As example, the incidence matrix and the admittance matrix for the system of figure 2.1 are composed hereunder.

1. The incidence matrix is a L×N-matrix with $\mathrm{a}_{l,n} = 1$ if line L starts at node N, $\mathrm{a}_{l,n}$ = -1 if line L ends at node N and $\mathrm{a}_{l,n} = 0$ if line L is not incident to node N. For the example of figure 2.1, the incidence matrix is:

$$\mathbf{A} = \begin{bmatrix} 1 & -1 & 0 & 0 & 0 \\ 1 & 0 & -1 & 0 & 0 \\ 0 & 1 & 0 & -1 & 0 \\ 0 & 0 & 1 & -1 & 0 \\ 0 & 0 & 1 & 0 & -1 \\ 0 & 0 & 0 & 1 & -1 \end{bmatrix} \tag{2.4}$$

2. Kirchoff's current law at each node:

$$\begin{aligned} \underline{I}_1 &= \underline{I}_{12} + \underline{I}_{13} \\ \underline{I}_2 &= -\underline{I}_{12} + \underline{I}_{24} \\ \underline{I}_3 &= -\underline{I}_{13} + \underline{I}_{34} + \underline{I}_{35} \\ \underline{I}_4 &= -\underline{I}_{24} - \underline{I}_{34} + \underline{I}_{45} \\ \underline{I}_5 &= -\underline{I}_{35} - \underline{I}_{45} \end{aligned}$$

$$or \quad \begin{bmatrix} \underline{I}_1 \\ \underline{I}_2 \\ \underline{I}_3 \\ \underline{I}_4 \\ \underline{I}_5 \end{bmatrix} = \mathbf{A}^T \cdot \begin{bmatrix} \underline{I}_{12} \\ \underline{I}_{13} \\ \underline{I}_{24} \\ \underline{I}_{34} \\ \underline{I}_{35} \\ \underline{I}_{45} \end{bmatrix} \quad or \quad \mathbf{i}_N = \mathbf{A}^T \cdot \mathbf{i}_L \tag{2.5}$$

3. Kirchoff's voltage law over each transmission line:

$$\begin{aligned}
(\underline{V}_1 - \underline{V}_2) \cdot \underline{Y}_{12} &= \underline{I}_{12} \\
(\underline{V}_1 - \underline{V}_3) \cdot \underline{Y}_{13} &= \underline{I}_{13} \\
(\underline{V}_2 - \underline{V}_4) \cdot \underline{Y}_{24} &= \underline{I}_{24} \\
(\underline{V}_3 - \underline{V}_4) \cdot \underline{Y}_{34} &= \underline{I}_{34} \\
(\underline{V}_3 - \underline{V}_5) \cdot \underline{Y}_{35} &= \underline{I}_{35} \\
(\underline{V}_4 - \underline{V}_5) \cdot \underline{Y}_{45} &= \underline{I}_{45}
\end{aligned} \tag{2.6}$$

$$or \quad \begin{bmatrix} \underline{V}_{12} \\ \underline{V}_{13} \\ \underline{V}_{24} \\ \underline{V}_{34} \\ \underline{V}_{35} \\ \underline{V}_{45} \end{bmatrix} = \mathbf{A} \cdot \begin{bmatrix} \underline{V}_1 \\ \underline{V}_2 \\ \underline{V}_3 \\ \underline{V}_4 \\ \underline{V}_5 \end{bmatrix} = \begin{bmatrix} \underline{I}_{12}/\underline{Y}_{12} \\ \underline{I}_{13}/\underline{Y}_{13} \\ \underline{I}_{24}/\underline{Y}_{24} \\ \underline{I}_{34}/\underline{Y}_{34} \\ \underline{I}_{35}/\underline{Y}_{35} \\ \underline{I}_{45}/\underline{Y}_{45} \end{bmatrix} \quad or \quad \mathbf{v}_L = \mathbf{A} \cdot \mathbf{v}_N$$

4. Substitution of Kirchoff's voltage law (equation 2.6) in Kirchoff's current law (equation 2.5) gives :

$$\begin{bmatrix} \underline{I}_1 \\ \underline{I}_2 \\ \underline{I}_3 \\ \underline{I}_4 \\ \underline{I}_5 \end{bmatrix} = \begin{bmatrix} \underline{Y}_{12} + \underline{Y}_{13} & -\underline{Y}_{12} & -\underline{Y}_{13} & 0 & 0 \\ -\underline{Y}_{12} & \underline{Y}_{12} + \underline{Y}_{24} & 0 & -\underline{Y}_{24} & 0 \\ -\underline{Y}_{13} & 0 & \underline{Y}_{13} + \underline{Y}_{34} + \underline{Y}_{35} & -\underline{Y}_{34} & -\underline{Y}_{35} \\ 0 & -\underline{Y}_{24} & -\underline{Y}_{34} & \underline{Y}_{24} + \underline{Y}_{34} + \underline{Y}_{45} & -\underline{Y}_{45} \\ 0 & 0 & -\underline{Y}_{35} & -\underline{Y}_{45} & \underline{Y}_{35} + \underline{Y}_{45} \end{bmatrix} \cdot \begin{bmatrix} \underline{V}_1 \\ \underline{V}_2 \\ \underline{V}_3 \\ \underline{V}_4 \\ \underline{V}_5 \end{bmatrix}$$

$$or \quad \mathbf{i}_N = \mathbf{Y} \cdot \mathbf{v}_N \tag{2.7}$$

In general, the admittance matrix of a network can be written as

$$\begin{aligned}
\mathbf{Y} &= \left[\underline{y}_{N,N'} \right] \\
\underline{y}_{N,N} &= \sum_{N'} \underline{Y}_{N,N'} \\
\underline{y}_{N,N'} &= -\underline{Y}_{N,N'}
\end{aligned} \tag{2.8}$$

$\underline{Y}_{N,N'}$ refers to the admittance of the line between the nodes N and N'. The admittance matrix $\mathbf{Y}$ is related to the incidence matrix $\mathbf{A}$ as follows

$$\mathbf{Y} = \mathbf{A}^T \cdot \mathbf{Y}_d \cdot \mathbf{A} \tag{2.9}$$

with $\mathbf{Y}_d$ a L×L-diagonal matrix with the line admittances on the diagonal (i.e., the primitive admittance matrix).

If two nodes are not connected, the impedance between these two nodes is infinite and the admittance is zero. Typically, a node is only connected to a limited number of other nodes, resulting in a sparse admittance matrix. If more than one transmission line between the same

two nodes exists, the admittance of these transmission lines can be simply added to an equivalent admittance. Grid elements like transformers can be incorporated in the grid description by their equivalent impedance. Often, an electricity grid is described in per-unit values, meaning that every grid parameter is expressed relative to a basis value.

Chapter 3

DC power flow

The most common calculation of the (static) grid flows and grid injections is the AC power flow. However, an AC power flow is computationally heavy within the scope of unit commitment models. An electricity grid with N nodes results in an AC power flow with 2N non-linear equations which have to be solved iteratively for each time step (see appendix 8 for the AC power flow equations). The high level of detail given by an AC power flow analysis does not always offset the computational effort. Therefore, a simplified version of the AC power flow can be used in unit commitment models; the DC power flow. This section gives a detailed description of DC power flows, based on the Ph.D. thesis from Purchala [2].

3.1 DC power flow assumptions

A DC power flow is a linearization of an AC power flow, based on three assumptions.

1. Line resistances are negligible compared to line reactances ($R_L << X_L$, for all lines). This assumption implies that grid losses are neglected and line parameters are simplified.

$$\begin{aligned} G_L &= \frac{R_L}{{R_L}^2 + {X_L}^2} \approx 0 \\ B_L &= \frac{-X_L}{{R_L}^2 + {X_L}^2} \approx -\frac{1}{X_L} \\ \underline{Z}_L \approx j \cdot X_L \qquad & \underline{Y}_L \approx j \cdot B_L \end{aligned} \tag{3.1}$$

   The diagonal matrix with line admittances $\mathbf{Y}_d$ can now be written as a diagonal matrix with line susceptances $\mathbf{B}_d$.

2. The voltage profile is flat, meaning that the voltage amplitude is equal for all nodes (in per unit values).

$$|V_N| \approx 1\, p.u. \tag{3.2}$$

3. Voltage angle differences between neighboring nodes are small. This assumption results in a linearization of the sine and cosine terms in the AC power flow equations.

$$\begin{aligned} \sin(\delta_N - \delta_Q) &\approx \delta_N - \delta_Q \\ \cos(\delta_N - \delta_Q) &\approx 1 \end{aligned} \tag{3.3}$$

The more these assumptions correspond to the reality, the more accurate the DC power flow solution is. DC power flow only considers active power flows, assumes perfect voltage support and reactive power management, and neglects transmission losses.

The DC power flow is a linearization of the non-linear AC power flow and therefore the reference point of the linearization has an impact. However, it is both empirically and theoretically shown in the literature that the DC power flow equations are relative insensitive to the operating point [3][4]. So in practice, one can use the same DC power flow equations for all possible operating points of the grid as long as the grid topology is retained.

3.2 DC power flow equations

The active power flow through a lossless transmission line is given by

$$P_L = \frac{|V_N||V_Q|}{X_L} \, sin(\delta_N - \delta_Q) \tag{3.4}$$

With the DC power flow assumptions in mind, equation 3.4 simplifies to the DC power flow equation for line flows (respectively for one line and in matrix form for all lines).

$$\begin{aligned} P_L &= B_L \left(\delta_N - \delta_Q\right) \\ \mathbf{p}_L &= \mathbf{B}_d \cdot \mathbf{A} \cdot \boldsymbol{\delta}_N \end{aligned} \tag{3.5}$$

The static AC power flow equation for active power injections at a node (see equation 8.3 in appendix) simplifies to the DC power flow equation for nodal active power balances (respectively for one node and in matrix format for all nodes).

$$\begin{aligned} P_N &= \sum_Q B_L \left(\delta_N - \delta_Q\right) \\ \mathbf{p}_N &= \mathbf{A}^T \cdot \mathbf{B}_d \cdot \mathbf{A} \cdot \boldsymbol{\delta}_N \end{aligned} \tag{3.6}$$

The positive direction of the active power flow P_L is from node N to node Q and B_L refers to the susceptance of line L between node N and node Q.

Substituting the nodal voltage angles δ_N from equations 3.5 and 3.6 gives the DC power flow equations.

$$\mathbf{p}_L = \left((\mathbf{B}_d \cdot \mathbf{A}) \cdot (\mathbf{A}^T \cdot \mathbf{B}_d \cdot \mathbf{A})^{-1}\right) \cdot \mathbf{p}_N \tag{3.7}$$

with

$$\mathbf{PTDF}^{L \times N} = (\mathbf{B}_d \cdot \mathbf{A}) \cdot (\mathbf{A}^T \cdot \mathbf{B}_d \cdot \mathbf{A})^{-1} \tag{3.8}$$

The DC power flow equations for nodal power balances (equations 3.6) are linearly dependent. As a result, the matrix $(\mathbf{A}^T \cdot \mathbf{B}_d \cdot \mathbf{A})$ is singular and its inverse does not exist. To overcome this issue, (at least) one node has to be designated as reference node and removed from the DC power flow equations. In the matrix $(\mathbf{B}_d \cdot \mathbf{A})$ the column corresponding to the reference node has to be removed while in the matrix $(\mathbf{A}^T \cdot \mathbf{B}_d \cdot \mathbf{A})$ both the column and row corresponding to the reference node have to be removed. With respect to voltage angles, only the difference in voltage angles between two neighboring nodes matters. Therefore the voltage angle of the reference node is set to zero. Finally, one additional relationship has to be added to the set

of equations to make sure that the DC power flow has one unique solution. This relationship expresses that the sum of all nodal injections equals zero.

$$\sum_{N} P_N = 0 \tag{3.9}$$

The Power Transfer Distribution Factor matrix (PTDF-matrix) describes the linear relationship between the power injections in the grid ($\mathbf{p}_N$) and the active power flows through the transmission lines ($\mathbf{p}_L$). An element $ptdf_{L,N}$ of the PTDF-matrix gives the power flow through transmission line L caused by the injection of 1 unit active power at node N and withdrawal of this active power at the reference node. Due to the linear character of the PTDF-matrix, the line flow at line L caused by an injection at node N with withdrawal at node Q, can be written as the difference in the line flow in L due to an injection at node N with withdrawal at the reference node and the line flow in L due to an injection at node Q with withdrawal at the reference node. In the final PTDF-matrix, the column corresponding to the reference node is a zero column.

During the PTDF calculation, at least one node has to be removed from the DC power flow equations to make the set of equations linearly independent (i.e., the reference node). Mathematically, the number of reference nodes can be determined as the difference between the number of nodes in the grid and the number of linearly independent columns in the incidence matrix of the grid. In a connected grid with only AC lines, one reference node is required to calculate the PTDF-matrix with equation 3.8. In a connected grid with both AC and DC lines, it might happen that a sub-grid of AC lines exists which is connected to the rest of the grid only via a DC line (see upper panel of figure 3.1). In this case, one reference node for each sub-grid is required to calculate the PTDF-matrix with equation 3.8. If the DC line is part of a meshed grid (instead of connecting two AC grids), one reference node for the whole grid is sufficient to calculate the PTDF-matrix. In a disconnected grid, at least two completely separated sub-grids exists (see lower panel of figure 3.1). In this case, one reference node for each sub-grid is required to calculate the PTDF-matrix with equation 3.8. Moreover, equation 3.9 has to be split up for every sub-grid.

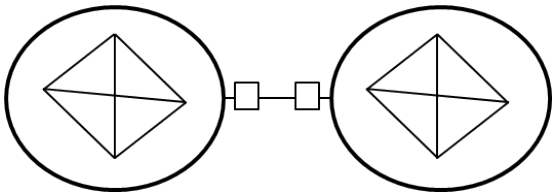

(a) AC grid with a DC connection.

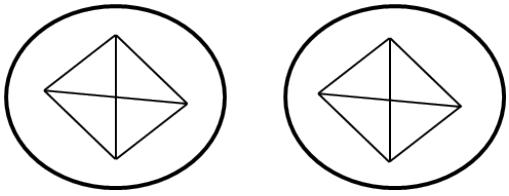

(b) Separated grids.

Figure 3.1: Illustration of the grid designs which require more than one reference node in the PTDF calculation.

In conclusion of this subsection, equation 3.7 and equation 3.9 give a closed mathematical relationship between grid injections and grid flows (DC power flow model). The active power

flows in the grid are limited by the transmission capacities of the lines.

$$\mathbf{p}_{L,min} \leq \mathbf{p}_L \leq \mathbf{p}_{L,max} \tag{3.10}$$

3.3 Correctness of DC power flow

The DC power flow is a linearization of the AC power flow based on three assumptions and hence by definition *incorrect*. The question is how incorrect a DC power flow is and whether the level of accuracy is acceptable or not. This section assesses the correctness of DC power flow compared with and AC power flow, based on the work of Purchala [2][5].

The first DC power flow simplification assumes lossless transmission lines (line resistance negligible compared to line reactances). The higher the voltage level of the considered grid, the more valid this assumption is. In the Belgian high voltage grid (900 lines from 70 kV to 380 kV), the average R/X ratio ranges from 0.10 at 380 kV to 0.32 at 70 kV. Purchala tested the correctness of this assumption on a 30-node test network and concluded that for R/X ratios below 0.50, the average error is always smaller than 5 % and falls below 2 % average error for R/X ratios below 0.20.

The second DC power flow simplification assumes a flat voltage profile. It is however almost impossible to avoid voltage fluctuations in an electricity grid. For small standard deviations in voltages (less than 0.01 p.u.), the average error[1] made by this assumption is limited to 5 %. However, realistic examples of voltage fluctuations in actual power systems show that this assumption is the most critical one and is the largest source of DC power flow errors.

The third DC power flow assumption is that voltage angle differences between neighboring nodes are small. In general, this assumption is more correct if the grid is weakly loaded. However, even during peak load, this assumption is justifiable in a meshed grid (e.g., the Belgian grid). For example, a winter peak load of 13 GW in the Belgian high voltage grid leads to a maximum voltage angle difference of 6°. In this case, which only occurs on a small number of lines, the fault made by linearization of the sine and cosine terms is less than 1 %.

In general, one can conclude that for high voltage grids - which are mostly the ones looked at in unit commitment models - the accuracy of DC power flows is around 5 %, compared to AC power flow and averaged over all lines. The deviation on single line flows can be much larger. Hence, the accuracy of DC power flow is acceptable in the scope of unit commitment models, but one should always keep the limitations of DC power flow in mind and be careful with drawing conclusions about single lines.

Note that the deviation between DC power flow simulations and the real grid flows is probably larger than the error made by using a linear DC grid model instead of a more accurate non-linear AC grid model. Simplifications of the grid topology (e.g. neglecting the distribution grid), assumptions on the grid topology (e.g. configuration of substations) and other input data related difficulties cause deviations between AC power flow simulations and reality.

[1]The error is defined as the relative differences in line flows between the AC power flow solution and the DC power flow solution, averaged over all lines.

3.4 Example of DC power flow

As illustration, the DC power flow equations are derived for the electricity grid of figure 2.1. For this simple grid, the DC power flow equations for line flows are (see equation 3.5)

$$\begin{aligned} P_{12} &= B_{12}\,(\delta_1 - \delta_2) \\ P_{13} &= B_{13}\,(\delta_1 - \delta_3) \\ P_{24} &= B_{24}\,(\delta_2 - \delta_4) \\ P_{34} &= B_{34}\,(\delta_3 - \delta_4) \\ P_{35} &= B_{35}\,(\delta_3 - \delta_5) \\ P_{45} &= B_{45}\,(\delta_4 - \delta_5) \end{aligned} \tag{3.11}$$

$$\begin{bmatrix} P_{12} \\ P_{13} \\ P_{24} \\ P_{34} \\ P_{35} \\ P_{45} \end{bmatrix} = \begin{bmatrix} B_{12} & -B_{12} & 0 & 0 & 0 \\ B_{13} & 0 & -B_{13} & 0 & 0 \\ 0 & B_{24} & 0 & -B_{24} & 0 \\ 0 & 0 & B_{34} & -B_{34} & 0 \\ 0 & 0 & B_{35} & 0 & -B_{35} \\ 0 & 0 & 0 & B_{45} & -B_{45} \end{bmatrix} \cdot \begin{bmatrix} \delta_1 \\ \delta_2 \\ \delta_3 \\ \delta_4 \\ \delta_5 \end{bmatrix}$$

The DC power flow equations for nodal power balances are (see equation 3.6)

$$\begin{aligned} P_1 &= B_{12}\,(\delta_1 - \delta_2) + B_{13}\,(\delta_1 - \delta_3) \\ P_2 &= B_{12}\,(\delta_2 - \delta_1) + B_{24}\,(\delta_2 - \delta_4) \\ P_3 &= B_{13}\,(\delta_3 - \delta_1) + B_{34}\,(\delta_3 - \delta_4) + B_{35}\,(\delta_3 - \delta_5) \\ P_4 &= B_{24}\,(\delta_4 - \delta_2) + B_{34}\,(\delta_4 - \delta_3) + B_{45}\,(\delta_4 - \delta_5) \\ P_5 &= B_{35}\,(\delta_5 - \delta_3) + B_{45}\,(\delta_5 - \delta_4) \end{aligned}$$

$$\begin{bmatrix} P_1 \\ P_2 \\ P_3 \\ P_4 \\ P_5 \end{bmatrix} = \begin{bmatrix} B_{12}+B_{13} & -B_{12} & -B_{13} & 0 & 0 \\ -B_{12} & B_{12}+B_{24} & 0 & -B_{24} & 0 \\ -B_{13} & 0 & B_{13}+B_{34}+B_{35} & -B_{34} & -B_{35} \\ 0 & -B_{24} & -B_{34} & B_{24}+B_{34}+B_{45} & -B_{45} \\ 0 & 0 & -B_{35} & -B_{45} & B_{35}+B_{45} \end{bmatrix} \cdot \begin{bmatrix} \delta_1 \\ \delta_2 \\ \delta_3 \\ \delta_4 \\ \delta_5 \end{bmatrix}$$

(3.12)

Let's take node 3 as reference node. Removing this reference node in equations 3.11 and 3.12 reduces these equations to

$$\begin{bmatrix} P_{12} \\ P_{13} \\ P_{24} \\ P_{34} \\ P_{35} \\ P_{45} \end{bmatrix} = \begin{bmatrix} B_{12} & -B_{12} & 0 & 0 \\ B_{13} & 0 & 0 & 0 \\ 0 & B_{24} & -B_{24} & 0 \\ 0 & 0 & -B_{34} & 0 \\ 0 & 0 & 0 & -B_{35} \\ 0 & 0 & B_{45} & -B_{45} \end{bmatrix} \cdot \begin{bmatrix} \delta_1 \\ \delta_2 \\ \delta_4 \\ \delta_5 \end{bmatrix} \tag{3.13}$$

$$\begin{bmatrix} P_1 \\ P_2 \\ P_4 \\ P_5 \end{bmatrix} = \begin{bmatrix} B_{12}+B_{13} & -B_{12} & 0 & 0 \\ -B_{12} & B_{12}+B_{24} & -B_{24} & 0 \\ 0 & -B_{24} & B_{24}+B_{34}+B_{45} & -B_{45} \\ 0 & 0 & -B_{45} & B_{35}+B_{45} \end{bmatrix} \cdot \begin{bmatrix} \delta_1 \\ \delta_2 \\ \delta_4 \\ \delta_5 \end{bmatrix}$$

The PTDF-matrix is given by

$$\mathbf{PTDF} = \begin{bmatrix} B_{12} & -B_{12} & 0 & 0 \\ B_{13} & 0 & 0 & 0 \\ 0 & B_{24} & -B_{24} & 0 \\ 0 & 0 & -B_{34} & 0 \\ 0 & 0 & 0 & -B_{35} \\ 0 & 0 & B_{45} & -B_{45} \end{bmatrix} \cdot \begin{bmatrix} B_{12}+B_{13} & -B_{12} & 0 & 0 \\ -B_{12} & B_{12}+B_{24} & -B_{24} & 0 \\ 0 & -B_{24} & B_{24}+B_{34}+B_{45} & -B_{45} \\ 0 & 0 & -B_{45} & B_{35}+B_{45} \end{bmatrix}^{-1} \tag{3.14}$$

Assume all line susceptances equal to 0.5 p.u. The PTDF-matrix becomes

$$\mathbf{PTDF} = \begin{bmatrix} 0.27 & -0.45 & 0 & -0.18 & -0.09 \\ 0.73 & 0.45 & 0 & 0.18 & 0.09 \\ 0.27 & 0.55 & 0 & -0.18 & -0.09 \\ -0.18 & -0.36 & 0 & -0.55 & -0.27 \\ -0.09 & -0.18 & 0 & -0.27 & -0.64 \\ 0.09 & 0.18 & 0 & 0.27 & -0.36 \end{bmatrix} \tag{3.15}$$

A zero column is added to the PTDF-matrix corresponding to the reference node. The PTDF-matrix shows, for example, that for an injection of 1 p.u. active power at node 1 (and off-take of this power at the reference node), 0.73 p.u. is flowing through line 13 and 0.27 p.u. through lines 12 and 24. This latter flow is divided among line 34 (0.18 p.u.) and lines 35 and 45 (0.09 p.u.).

Chapter 4

Power flow controlling devices in DC power flow

Power flow controlling (PFC) devices allow to control the active power flow through transmission lines. Power flow controlling devices are being categorized into two types: flexible AC transmission systems (FACTS, e.g., phase shifting transformers) and high voltage DC lines (HVDC). This section gives an overview of power flow controlling devices and their representation in DC power flow networks, based on the Ph.D. thesis of Van Hertem [6] and the Ph.D. thesis of Verboomen [7].

Recall that the power flow through a lossless transmission line is given by

$$P_L = \frac{|V_N||V_Q|}{X_L} \, sin(\delta_N - \delta_Q) \tag{4.1}$$

From equation 4.1, it becomes clear that the power flow through a line can be controlled by changing the line impedance X_L or the voltage angle difference $(\delta_N - \delta_Q)$. The voltage magnitudes $|V_N|$ and $|V_Q|$ can not be used to control active power flows as they need to stay close to their predefined value to ensure a safe grid operation. Altering the line impedance can be achieved by means of a mechanically switched series capacitor, a thyristor controlled series compensator, a static synchronous series compensator or fixed series compensation. These devices can be modeled as a variable line impedance. Altering the voltage angle difference between two nodes can be achieved by means of a phase shifting transformer (PST). A PST creates a voltage angle shift by inserting a voltage in quadrature to the phase voltage. All devices mentioned in this paragraph are examples of FACTS.

As part of a meshed grid, high voltage direct current (HVDC) lines can also be considered as power flow devices. The power flow through a HVDC line can be fully controlled by the AC-DC/DC-AC converters at its ends. If a HVDC is used for a point-to-point connection (e.g. connecting offshore wind turbines with the onshore grid or interconnection between two asynchronous power systems), than the HVDC link is not a true power flow controlling device. Only if embedded in a meshed grid, a HVDC link can be used as power flow controlling device.

In the remainder of this section, phase shifting transformers and HVDC lines are discussed in detail. The focus is on how these grid elements can be modeled in a DC power flow.

4.1 Phase shifting transformers

Resume the DC power flow equations for line flows (see equation 3.5) and for nodal active power balances (see equation 3.6). A phase shifting transformer (PST) at line L changes the voltage angle between the two adjacent nodes N and Q with angle α_L. The DC power flow equations for line flows, respectively for one line and in matrix form for all lines, become

$$\begin{aligned} P_L &= B_L \left(\delta_N - \delta_Q + \alpha_L\right) \\ \mathbf{p}_L &= \mathbf{B}_d \cdot \mathbf{A} \cdot \boldsymbol{\delta}_N + \mathbf{B}_d \cdot \boldsymbol{\alpha}_L \end{aligned} \tag{4.2}$$

The DC power flow equation for nodal active power balances, respectively for one node and in matrix form for all nodes, become

$$\begin{aligned} P_N &= \sum_Q B_L \left(\delta_N - \delta_Q + \alpha_L\right) \\ \mathbf{p}_N &= \mathbf{A}^T \cdot \mathbf{B}_d \cdot \mathbf{A} \cdot \boldsymbol{\delta}_N + \left(\mathbf{B}_d \cdot \mathbf{A}\right)^T \cdot \boldsymbol{\alpha}_L \end{aligned} \tag{4.3}$$

Substituting the nodal voltage angles δ_N from equations 4.2 and 4.3 gives

$$\begin{aligned} \mathbf{p}_L = &\left(\left(\mathbf{B}_d \cdot \mathbf{A}\right) \cdot \left(\mathbf{A}^T \cdot \mathbf{B}_d \cdot \mathbf{A}\right)^{-1}\right) \cdot \mathbf{p}_N + \\ &\left(\mathbf{B}_d - \left(\mathbf{B}_d \cdot \mathbf{A}\right) \cdot \left(\mathbf{A}^T \cdot \mathbf{B}_d \cdot \mathbf{A}\right)^{-1} \cdot \left(\mathbf{B}_d \cdot \mathbf{A}\right)^T\right) \cdot \boldsymbol{\alpha}_L \end{aligned} \tag{4.4}$$

with the PTDF-matrix the same as in the basic DC power flow

$$\mathbf{PTDF}^{L \times N} = \left(\mathbf{B}_d \cdot \mathbf{A}\right) \cdot \left(\mathbf{A}^T \cdot \mathbf{B}_d \cdot \mathbf{A}\right)^{-1} \tag{4.5}$$

and with Phase Shifter Distribution Factors (PSDF) given by

$$\mathbf{PSDF}^{L \times L'} = \mathbf{B}_d - \left(\mathbf{B}_d \cdot \mathbf{A}\right) \cdot \left(\mathbf{A}^T \cdot \mathbf{B}_d \cdot \mathbf{A}\right)^{-1} \cdot \left(\mathbf{B}_d \cdot \mathbf{A}\right)^T \tag{4.6}$$

Each element in the PSDF-matrix $psdf_{L,L'}$ gives the impact of a change of one radian in the PST angle at line L' on the flow through transmission line L. The concept of the PSDF-matrix is thus completely analogous to the PTDF-matrix. Note that in the equations above, it is assumed that a positive PST angle increases the power flow in the positive direction through the line where the PST is located. The reverse assumption is possible as well, depending on the sign convention. The mathematical derivation is done for a grid with a PST on each line. In reality, mostly only a few lines in a grid are equipped with a PST. In that case, only the columns in the PSDF-matrix corresponding to lines with a PST are useful and the other columns can be removed. In order to calculate the PSDF-matrix, a reference node has to be chosen. However, unlike the PTDF-matrix, the PSDF-matrix looks exactly the same for every possible reference node.

The range of possible phase shifter angles is limited. Phase shifting transformers are typically operated in the range ± 30° (± 25° in Belgium).

$$\boldsymbol{\alpha}_{L,min} \leq \boldsymbol{\alpha}_L \leq \boldsymbol{\alpha}_{L,max} \tag{4.7}$$

Retake the example from figure 2.1 and let's derive the full PSDF-matrix. The DC power flow equations for line flows are

$$
\begin{aligned}
P_{12} &= B_{12}\left(\delta_1 - \delta_2 + \alpha_{12}\right) \\
P_{13} &= B_{13}\left(\delta_1 - \delta_3 + \alpha_{13}\right) \\
P_{24} &= B_{24}\left(\delta_2 - \delta_4 + \alpha_{24}\right) \\
P_{34} &= B_{34}\left(\delta_3 - \delta_4 + \alpha_{34}\right) \\
P_{35} &= B_{35}\left(\delta_3 - \delta_5 + \alpha_{35}\right) \\
P_{45} &= B_{45}\left(\delta_4 - \delta_5 + \alpha_{45}\right)
\end{aligned}
$$

$$
\begin{bmatrix} P_{12} \\ P_{13} \\ P_{24} \\ P_{34} \\ P_{35} \\ P_{45} \end{bmatrix} = \begin{bmatrix} B_{12} & -B_{12} & 0 & 0 & 0 \\ B_{13} & 0 & -B_{13} & 0 & 0 \\ 0 & B_{24} & 0 & -B_{24} & 0 \\ 0 & 0 & B_{34} & -B_{34} & 0 \\ 0 & 0 & B_{35} & 0 & -B_{35} \\ 0 & 0 & 0 & B_{45} & -B_{45} \end{bmatrix} \cdot \begin{bmatrix} \delta_1 \\ \delta_2 \\ \delta_3 \\ \delta_4 \\ \delta_5 \end{bmatrix} + \tag{4.8}
$$

$$
\begin{bmatrix} B_{12} & 0 & 0 & 0 & 0 & 0 \\ 0 & B_{13} & 0 & 0 & 0 & 0 \\ 0 & 0 & B_{24} & 0 & 0 & 0 \\ 0 & 0 & 0 & B_{34} & 0 & 0 \\ 0 & 0 & 0 & 0 & B_{35} & 0 \\ 0 & 0 & 0 & 0 & 0 & B_{45} \end{bmatrix} \cdot \begin{bmatrix} \alpha_{12} \\ \alpha_{13} \\ \alpha_{24} \\ \alpha_{34} \\ \alpha_{35} \\ \alpha_{45} \end{bmatrix}
$$

The DC power flow equations for nodal power balances are

$$
\begin{aligned}
P_1 &= B_{12}\left(\delta_1 - \delta_2 + \alpha_{12}\right) + B_{13}\left(\delta_1 - \delta_3 + \alpha_{13}\right) \\
P_2 &= B_{12}\left(\delta_2 - \delta_1 - \alpha_{12}\right) + B_{24}\left(\delta_2 - \delta_4 + \alpha_{24}\right) \\
P_3 &= B_{13}\left(\delta_3 - \delta_1 - \alpha_{13}\right) + B_{34}\left(\delta_3 - \delta_4 + \alpha_{34}\right) + B_{35}\left(\delta_3 - \delta_5 + \alpha_{35}\right) \\
P_4 &= B_{24}\left(\delta_4 - \delta_2 - \alpha_{24}\right) + B_{34}\left(\delta_4 - \delta_3 - \alpha_{34}\right) + B_{45}\left(\delta_4 - \delta_5 + \alpha_{45}\right) \\
P_5 &= B_{35}\left(\delta_5 - \delta_3 - \alpha_{35}\right) + B_{45}\left(\delta_5 - \delta_4 - \alpha_{45}\right)
\end{aligned}
$$

$$
\begin{bmatrix} P_1 \\ P_2 \\ P_3 \\ P_4 \\ P_5 \end{bmatrix} = \begin{bmatrix} B_{12}+B_{13} & -B_{12} & -B_{13} & 0 & 0 \\ -B_{12} & B_{12}+B_{24} & 0 & -B_{24} & 0 \\ -B_{13} & 0 & B_{13}+B_{34}+B_{35} & -B_{34} & -B_{35} \\ 0 & -B_{24} & -B_{34} & B_{24}+B_{34}+B_{45} & -B_{45} \\ 0 & 0 & -B_{35} & -B_{45} & B_{35}+B_{45} \end{bmatrix} \cdot \begin{bmatrix} \delta_1 \\ \delta_2 \\ \delta_3 \\ \delta_4 \\ \delta_5 \end{bmatrix}
$$

$$
+ \begin{bmatrix} B_{12} & B_{13} & 0 & 0 & 0 & 0 \\ -B_{12} & 0 & B_{24} & 0 & 0 & 0 \\ 0 & -B_{13} & 0 & B_{34} & B_{35} & 0 \\ 0 & 0 & -B_{24} & -B_{34} & 0 & B_{45} \\ 0 & 0 & 0 & 0 & -B_{35} & -B_{45} \end{bmatrix} \cdot \begin{bmatrix} \alpha_{12} \\ \alpha_{13} \\ \alpha_{24} \\ \alpha_{34} \\ \alpha_{35} \\ \alpha_{45} \end{bmatrix} \tag{4.9}
$$

Let's take node 3 again as reference node, which implies that P_3 and δ_3 are removed from equations 4.8 and 4.9. The PTDF-matrix is the same as in the example without PSTs (see equation 3.14). The PSDF-matrix is given by equation 4.6. Assume all line susceptances equal

to 0.5 p.u. The PSDF-matrix becomes

$$\mathbf{PSDF} = \begin{bmatrix} 0.14 & -0.14 & 0.14 & -0.09 & -0.05 & 0.05 \\ -0.14 & 0.14 & -0.14 & 0.09 & 0.05 & -0.05 \\ 0.14 & -0.14 & 0.14 & -0.09 & -0.05 & 0.05 \\ -0.09 & 0.09 & -0.09 & 0.23 & -0.14 & 0.14 \\ -0.05 & 0.05 & -0.05 & -0.14 & 0.18 & -0.18 \\ 0.05 & -0.05 & 0.05 & 0.14 & -0.18 & 0.18 \end{bmatrix} \tag{4.10}$$

The elements of the PSDF-matrix are expressed in power flow in [p.u.] per phase shift angle in [radian]. The PSDF-matrix can be converted to [MW/°] by multiplying the original PSDF-matrix with the power base (in MW) divided by 57.3[1].

The PSDF-matrix indicates that an increase in the PST angle at line A with 1 radian increases the flow through line A with 0.14 p.u. As a results, the flows through lines B is decreased with 0.14 p.u. and the flow through line C increased with 0.14 p.u. This causes also flow changes in lines D, E and F of respectively -0.09 p.u., -0.05 p.u. and 0.05 p.u.

The DC power flow representation of PSTs causes an extra inaccuracy, on top of the inaccuracy of the basic DC power flow. Overall, the error introduced by an approximate PST model is small. This error increases with higher phase shift angles, up to about 5 % at maximum phase shift angles. This 5 % accuracy adds up to the 5 % accuracy of the basic DC power flow, ending up with a 5-10 % accuracy of DC power flow with PSTs. Once again, the DC power flow is useful in unit commitment modeling but one should always keep the limitations of DC power flow in mind [8].

4.2 High voltage direct current lines

Up until now, only AC transmission lines were considered. This subsection describes how high voltage direct current (HVDC) lines can be incorporated in the grid model. The power flow through a HVDC line is fully controllable. Hence, a HVDC link can be modeled as a combination of a controllable positive and negative power injection at the sending and receiving end of the link. The flow through the HVDC link affects the flows in the AC lines. Therefore, an additional term has to be added to the DC power flow equations of the AC lines.

Retake the DC power flow equations for the AC grid including PSTs (see equations 4.4, 4.5 and 4.6). The subscript AC is added to emphasize that we are dealing with AC lines.

$$\mathbf{p}_{L,AC} = \mathbf{PTDF} \cdot \mathbf{p}_{N,AC} + \mathbf{PSDF} \cdot \boldsymbol{\alpha}_{L,AC} \tag{4.11}$$

So far, all nodal injections P_N were injected in the AC grid. With DC lines in the grid, some of the injected power will flow through the HVDC grid and some through the AC grid.

$$\mathbf{p}_{N,AC} = \mathbf{p}_N - \mathbf{p}_{N,DC} \tag{4.12}$$

The flow through each HVDC line can be fully controlled. The relationship between the active power flows through the HVDC lines $\mathrm{P}_{L,DC}$ and the nodal injections $\mathrm{P}_{N,DC}$ is given by

$$\mathbf{p}_{N,DC} = \mathbf{A}_{DC}^T \cdot \mathbf{p}_{L,DC} \tag{4.13}$$

[1] One radian is equivalent with 57.3°.

with $\mathbf{A}_{DC}$ the incidence matrix of the HVDC network. The combination of equations 4.11, 4.12 and 4.13 gives the DC power flow equations for a network with PSTs, AC lines and DC lines.

$$\mathbf{p}_{L,AC} = \mathbf{PTDF} \cdot \mathbf{p}_N + \mathbf{PSDF} \cdot \boldsymbol{\alpha}_{L,AC} + \mathbf{DCDF} \cdot \mathbf{p}_{L,DC} \tag{4.14}$$

with the Direct Current Distribution Factors (DCDF)

$$\mathbf{DCDF} = -\mathbf{PTDF} \cdot \ \mathbf{A}_{DC}^T \tag{4.15}$$

Each element in the DCDF-matrix $dcdf_{L_{ac},L_{dc}}$ gives the impact of the controllable power flow in the DC line L_{dc} at the power flow in the AC line L_{ac}. The concept of the DCDF-matrix is analogous to the PTDF-matrix and the PSDF-matrix. Equation 4.14 has to be solved for the flows in the AC lines. The other grid parameters (nodal grid injections, phase shifter angles and flows in the DC lines) are input parameters for this grid equation, implicit to the model.

Retake the network from figure 2.1 and assume that line 12 and 45 are HVDC lines (see figure 4.1).

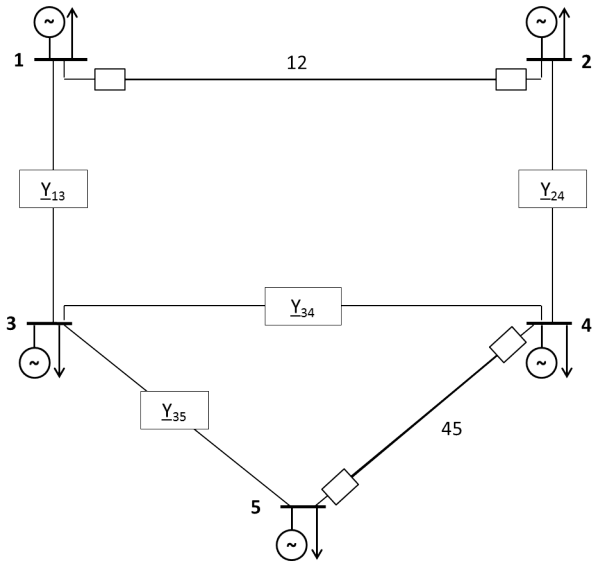

Figure 4.1: Electricity grid with 5 nodes and 6 transmission lines with line 12 and 45 HVDC links.

The incidence matrices for the AC network and DC network become

$$\mathbf{A}_{AC} = \begin{bmatrix} 1 & 0 & -1 & 0 & 0 \\ 0 & 1 & 0 & -1 & 0 \\ 0 & 0 & 1 & -1 & 0 \\ 0 & 0 & 1 & 0 & -1 \end{bmatrix}, \ \mathbf{A}_{DC} = \begin{bmatrix} 1 & -1 & 0 & 0 & 0 \\ 0 & 0 & 0 & 1 & -1 \end{bmatrix} \tag{4.16}$$

The PTDF-matrix of the AC network follows from equation 3.8. With node 3 as reference node, the PTDF-matrix is

$$\mathbf{PTDF} = \begin{bmatrix} 1 & 0 & 0 & 0 & 0 \\ 0 & 1 & 0 & 0 & 0 \\ 0 & -1 & 0 & -1 & 0 \\ 0 & 0 & 0 & 0 & -1 \end{bmatrix} \tag{4.17}$$

The DCDF-matrix for the considered example follows from equation 4.15.

$$\mathbf{DCDF} = \begin{bmatrix} -1 & 0 \\ 1 & 0 \\ -1 & 1 \\ 0 & -1 \end{bmatrix} \tag{4.18}$$

The resulting DC power flow equations, in a network without PSTs, are

$$\begin{bmatrix} P_{13} \\ P_{24} \\ P_{34} \\ P_{35} \end{bmatrix} = \begin{bmatrix} 1 & 0 & 0 & 0 & 0 \\ 0 & 1 & 0 & 0 & 0 \\ 0 & -1 & 0 & -1 & 0 \\ 0 & 0 & 0 & 0 & -1 \end{bmatrix} \cdot \begin{bmatrix} P_1 \\ P_2 \\ P_3 \\ P_4 \\ P_5 \end{bmatrix} + \begin{bmatrix} -1 & 0 \\ 1 & 0 \\ -1 & 1 \\ 0 & -1 \end{bmatrix} \cdot \begin{bmatrix} P_{12} \\ P_{45} \end{bmatrix} \tag{4.19}$$

P_{12} and P_{45} are flows through HVDC links and are thus controllable.

DC transmission losses can be incorporated by setting a difference between the injection at the sending end and the injection at the receiving end.

Chapter 5

Nodal and zonal models in DC power flow

One distinguishes two different types of grid models based on the level of granularity: nodal grid models and zonal grid models. In nodal models, each – relevant – node and line is included. Nodal grid models describe the grid with a high level of accuracy, but their practical use is rather limited. Nodal grid models require detailed input data (e.g., exact location of each power plant) and cause relative long run times. In zonal grid models, different nodes are grouped into zones and represented by equivalent nodes. Similarly, transmission lines between zones are aggregated to equivalent inter-zonal links while intra-zonal lines are omitted from the model[1]. Obviously, reducing nodal models to zonal models goes together with a loss in accuracy. The advantage of zonal grid models is the relative simplicity, in the sense that fewer grid constraints have to be taken into account and system data only has to be known on an aggregated level (e.g., installed generation capacity per zone instead of per node). In summary, the difference between nodal and zonal grid models comes down to finding a balance between accuracy (i.e., taking account of all grid constraints) and convenience (i.e., usefulness of the grid model in real-life applications). In the literature, a lively and extensive discussion on this matter can be found (see for example [9]).

Figure 5.1 illustrates a nodal-zonal grid reduction. The original nodal grid model (5 nodes and 6 lines) is reduced to a zonal grid model (3 zones and 3 lines). The reduction from a nodal to a zonal grid model must be performed for two dimensions: power flows in the grid and transmission capacities of lines. These two dimensions will be consecutively dealt with in more detail.

5.1 Nodal-zonal reduction: power flows

A nodal grid model is characterized by a nodal PTDF-matrix, containing the relation between nodal grid injections and power flows through the transmission lines. Analogously, a zonal grid model is characterized by a zonal PTDF-matrix, containing the relation between zonal grid

[1] Nodal and zonal are relative concepts rather than absolute concepts, depending on the scope of the analysis. For example, in a European grid study, a nodal grid model might include all nodes and transmission lines above 200 kV while a in a zonal network model each country is represented by one equivalent node. On the other hand, in a Belgian grid study a nodal model might cover all voltage levels while the zonal model is limited to voltage levels above 200 kV.

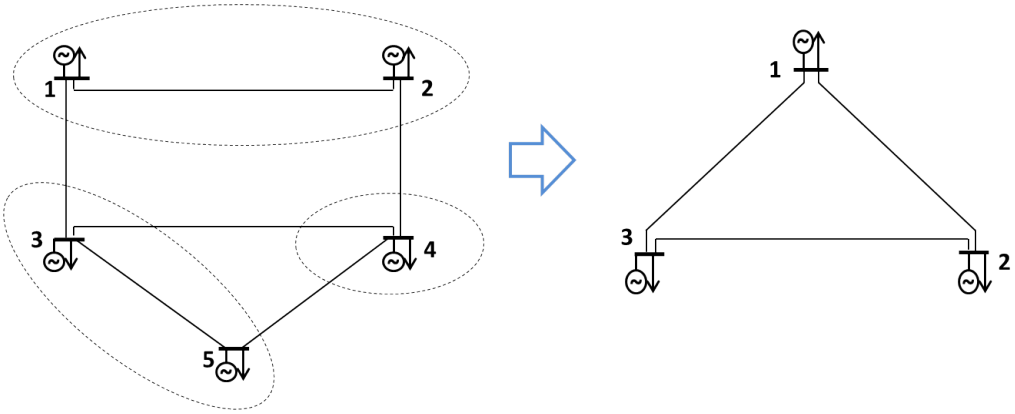

Figure 5.1: The original nodal electricity grid is reduced to a zonal grid model.

injections and power flows through the equivalent lines. This section explains how the zonal PTDF-matrix is derived from the nodal PTDF-matrix.

With regard to the reduction from nodal flows to zonal flows, the zonal DC power flow model (zonal PTDF-matrix) can be derived from the nodal grid model based on two different approaches. According to the first approach, the zonal PTDF-matrix is composed based on different nodal DC power flow simulations. A first power flow simulation represents the reference case. All other power flows represent deviations from this reference case, in which the zonal balance of one zone is increased (more generation) while the zonal balance of the reference zone is decreased (more load). The zonal PTDFs can then be calculated as the difference in inter-zonal flows due to a change in the zonal balances (averaged out over the different power flows). The second approach derives the zonal PTDF-matrix directly from the nodal PTDF-matrix, based on row and column operations. This approach consists of 3 steps: (1) omitting the rows in the nodal PTDF-matrix corresponding to intra-zonal lines, (2) grouping different nodes into zones based on generation-shift keys and (3) adding flows in parallel inter-zonal lines into one cross-border line.

The nodal-zonal grid reduction for flows is demonstrated for the example in figure 5.1, using the matrix based approach. The nodal PTDF-matrix of the original nodal grid is (see also equation 3.15, all line susceptances equal to 0.5 p.u.)

$$\mathbf{PTDF}_{nodal} = \begin{bmatrix} 0.27 & -0.45 & 0 & -0.18 & -0.09 \\ 0.73 & 0.45 & 0 & 0.18 & 0.09 \\ 0.27 & 0.55 & 0 & -0.18 & -0.09 \\ -0.18 & -0.36 & 0 & -0.55 & -0.27 \\ -0.09 & -0.18 & 0 & -0.27 & -0.64 \\ 0.09 & 0.18 & 0 & 0.27 & -0.36 \end{bmatrix} \tag{5.1}$$

First, the rows in the nodal PTDF-matrix corresponding to intra-zonal lines are omitted from the matrix (i.e. lines 12 - first row - and 35 - fifth row). Second, the remaining PTDF-matrix is reduced to a zone-to-line PTDF-matrix by grouping nodes into zones. In this step, the generation shift keys (GSK) have to be known. GSKs indicate the nodal contribution to a change in the zonal generation balance. Assume for example that the GSKs for the example of figure 5.1 are

given by

$$\mathbf{GSK}^{N\times Z} = \begin{bmatrix} 1.5 & 0 & 0 \\ -0.5 & 0 & 0 \\ 0 & 0 & 0.5 \\ 0 & 1 & 0 \\ 0 & 0 & 0.5 \end{bmatrix} \tag{5.2}$$

This GSK-matrix shows that an increase with one unit in the zonal generation balance of zone 1 (nodes 1 and 2) comes from an increase in generation at node 1 with 1.5 unit and an increase in load at node 2 with 0.5 unit. Analogously for zone 3, where node 3 and node 5 contribute equally to a change in the zonal generation balance. As node 4 is the only node in zone 2, its generation shift key is 1. Note that the sum of each column in the GSK-matrix has to be 1. Three common approaches exist to determine the nodal contribution to an incremental zonal generation balance change, i.e., according to the merit order, based on the remaining available capacity or based on the production level [10]. In reality, no nodal solution is available ex-ante to calculate the generation shift keys. Therefore the generation shift keys have to be estimated based on historical system data. Moreover, GSKs change from time step to time step as the spatial distribution of load can change (e.g. winter versus summer, night versus day), just like the spatial distribution of generation (e.g. depending on wind conditions, power plant outages). The zone-to-line PTDF follows from

$$\mathbf{PTDF}_{nodal} \cdot \mathbf{GSK}^{N\times Z} = \mathbf{PTDF}_{zone-to-line}$$

$$\begin{bmatrix} 0.73 & 0.45 & 0 & 0.18 & 0.09 \\ 0.27 & 0.55 & 0 & -0.18 & -0.09 \\ -0.18 & -0.36 & 0 & -0.55 & -0.27 \\ 0.09 & 0.18 & 0 & 0.27 & -0.36 \end{bmatrix} \cdot \begin{bmatrix} 1.5 & 0 & 0 \\ -0.5 & 0 & 0 \\ 0 & 0 & 0.5 \\ 0 & 1 & 0 \\ 0 & 0 & 0.5 \end{bmatrix} = \begin{bmatrix} 0.87 & 0.18 & 0.05 \\ 0.13 & -0.18 & -0.05 \\ -0.09 & -0.55 & -0.13 \\ 0.05 & 0.27 & -0.18 \end{bmatrix} \tag{5.3}$$

In a third and last step, parallel flows between the same zones are added. One should pay attention to the sign convention. In this example, line 34 and line 45 both connect zone 2 with zone 3, but the positive direction of line 34 is opposite to the positive direction of the inter-zonal link 23. Therefore, the flow through line 34 has to be deducted from the flow through line 45 to calculate the flow through the inter-zonal link 23. The resulting zonal PTDF-matrix is

$$\mathbf{PTDF}_{zonal} = \begin{bmatrix} 0.87 & 0.18 & 0.05 \\ 0.13 & -0.18 & -0.05 \\ 0.14 & 0.82 & -0.05 \end{bmatrix} \tag{5.4}$$

In a zonal grid model, inter-zonal flows might occur when all zones are balanced (i.e., zero zonal grid injections). To take account of this effect, an extra term is added to the zonal DC power flow equations [11].

$$\mathbf{p}_{L,zonal} = \mathbf{PTDF}_{zonal} \cdot \mathbf{p}_{N,zonal} + \mathbf{p}^0_{L,zonal} \tag{5.5}$$

$\mathbf{p}^0_{L,zonal}$ is the inter-zonal flow at link L when each zone is balanced (i.e., the *zero imbalance* flows). The values for the *zero imbalance* flows can not be know ex-ante, but have to be estimated based on historical system data. Moreover, the *zero imbalance* flows vary in time, so in zonal grid models average values are being used.

The nodal-zonal grid reduction for flows is based on two assumptions. First, it is assumed that no congestion occurs within a zone and therefore the intra-zonal lines can be omitted from the grid model (see step 1 of the matrix operations). Second, it is assumed that the nodal distribution of generation and load within a zone is stationary (constant in time) and therefore the generation

shift keys are constant in time (see step 2 of the matrix operations). The accuracy of these assumptions depends on the grid design (i.e., a meshed grid versus a non-meshed grid), the operation of the power system (i.e., location of generating units and loads) and the granularity of the zonal grid model (i.e., the number of zones). The accuracy of the zonal grid model can be enhanced by increasing the granularity of the zonal grid model or by performing the grid reduction separately for different types of grid injections.

It is easy to understand that a higher level of granularity of the zonal grid (i.e., more zones) increases the accuracy of the grid model. The higher the number of zones, the smaller the zones are and hence the smaller the probability of intra-zonal congestion and the more constant the spatial distribution of generation and load within the zone. Increasing the zonal grid granularity thus increases the validity of both grid reduction assumptions. However, effectively increasing the granularity of the zonal model requires detailed knowledge of the grid as the zonal grid model should be composed in accordance with the design and operation of the grid. For example, two nodes connected by a transmission line which is often congested, should be allocated to different zones.

The accuracy of the zonal grid model can also be increased by performing the nodal-zonal grid reduction separately for different types of injections. Types of injections can refer to, for example, grid injections from nuclear power plants or grid off-takes from industrial consumers. The spatial distribution of one type of injections varies less in time than the spatial distribution of all injections together. In other words, generation shift keys of one type of grid injections are less variable in time than generation shift keys of all injections together. Grid reduction per type of injection thus increases the validity of the assumption on stationary spatial distribution of injections, but does not influence the assumption about intra-zonal congestion. In case of a zonal grid model with different nodal-zonal reductions per type of injection, the zonal DC power flow equations become

$$\mathbf{p}_{L,zonal} = \sum_{Y} \mathbf{PTDF}_{Y,zonal} \cdot \mathbf{p}_{Y,N,zonal} + \mathbf{p}^{0}_{L,zonal} \tag{5.6}$$

with $\mathbf{PTDF}_{Y,zonal}$ the zonal PTDF-matrix for injections of type Y and $\mathbf{p}_{Y,N,zonal}$ the zonal grid injection of type Y. The injections per type are limited to the zonal generation for production-related injections or to the zonal load for load-related off-takes;

$$\begin{aligned} 0 \leq p_{Y,N,zonal} \leq \sum_{i \in Y,N} g_i \qquad & \forall\, N, Y \in generation \\ 0 \leq -p_{Y,N,zonal} \leq \sum_{j \in Y,N} l_j \qquad & \forall\, N, Y \in load \end{aligned} \tag{5.7}$$

with g_i the power generation of power plant i and l_j the load of consumer j. Load causes grid off-takes (negative injections) and therefore the corresponding injections have to be non-positive. The net injection of the zone is the sum of all injections per type.

$$\mathbf{p}_{N,zonal} = \sum_{Y} \mathbf{p}_{Y,N,zonal} \tag{5.8}$$

5.2 Nodal-zonal reduction: line capacities

The power flow through a line is limited by its transmission capacity (see equation 3.10). In a nodal grid model, the transmission capacity of a line is simply determined by the physical

limits of the line. In a zonal grid model – where inter-zonal lines are aggregated into one inter-zonal link – it is less straightforward to determine the transmission capacities between zones. The transmission capacity of an aggregated inter-zonal line cannot be easily calculated as the sum of all separate transmission capacities, but depends on the operation of the whole grid (e.g., location of generating units and load) and the capacity calculation methodology (e.g., reliability margins) [12]. The cross-border capacity is determined by the Transmission System Operators (TSOs) according to a capacity allocation method. Two methods are possible: the Available Transmission Capacity (ATC) approach and the Flow-Based (FB) approach. The ATC approach provides one inter-zonal transmission capacity to the market for which a safe and secure operation of the grid is ensured. The ATC approach doesn't account for the flows at the other borders of the zone, which impact the capacity at the considered border. This implies that the ATC approach for capacity allocation conflicts with a DC power flow analysis. The FB approach takes account of the impact of the flows at the other borders and therefore the FB approach is less restrictive than the ATC approach in terms of the transmission capacity that is made available to the market. FB capacity allocation corresponds with a DC power flow grid model.

The transmission capacities imposed to zonal grid models do not always correspond to the real physical capacity limitations as imposed to the nodal grid model (depending on the capacity allocation mechanism). This difference in capacity constraints causes another deviation between nodal grid model and zonal grid model, on top of the deviations due to the assumption made in the flow reduction calculations (i.e., no intra-zonal congestion and stationary spatial distribution of load and generation).

Reliability considerations might be taken into account during the capacity allocation process (e.g., N-1 security constraint). Such reliability considerations reduce the transmission capacity for the market but increase the security margins to deal with contingencies.

Chapter 6

N-1 security in DC power flow

The N-1 security criterion is defined by CEER as the rule that the electric power network shall withstand the unplanned outage of one element in the system and stay in operation without jeopardizing system operational integrity [13]. The unplanned outage of one element may refer to the failure of a transmission line, transformer, generating unit or a busbar. Often the term *contingency* is used to denote the unplanned outage of one element in the system. The system status before this contingency is referred to as the pre-contingency state (N state), whereas the post-contingency refers to the system state after the contingency occurred (N-1 state).

Grid models that determine a N-1 secure operation of the grid are called security constrained optimal power flow models (SCOPF). A SCOPF is an optimal power flow (OPF) problem which takes into account constraints arising from the operation of the system under a set of postulated contingencies [14]. Note the difference between security constrained unit commitment (SCUC) and security constrained optimal power flow (SCOPF). SCUC models determine the optimal generation scheduling taking account of the grid constraints in the N state (mostly without considering contingencies). Generally speaking, the focus of SCUC models is on the generation units in the power system. SCOPF models determine the optimal system scheduling taking account of contingencies, with particular focus on the grid elements in the power system.

The N-1 security criterion has a preventive approach and a corrective approach. The preventive approach does not allow corrective actions after a contingency occurred, other than those that take place automatically (e.g., active power frequency control). The corrective approach does consider the possibility of corrective actions after a contingency occurred. Possible corrective actions are changing the power plant dispatch or the setting point of power flow controlling devices (phase shift transformers and HVDC lines).

In this text, the unplanned outages of transmission lines and transformers are dealt with. The failure of generation units are not considered. Note that N-1 security does only make sense in a nodal grid model in which each relevant transmission line and transformer is represented.

6.1 Mathematical formulation of N-1 security

The N-1 security criterion can be compactly formulated as follows [15]:

$$\min f(\mathbf{x}, \mathbf{u}_0) \tag{6.1}$$

$$g_0(\mathbf{x}, \mathbf{u}_0) = 0 \tag{6.2}$$

$$h_0(\mathbf{x}, \mathbf{u}_0) \leq 0 \tag{6.3}$$

$$g_k(\mathbf{x}, \mathbf{u}_k) = 0 \qquad k = 1, ..., K \tag{6.4}$$

$$h_k(\mathbf{x}, \mathbf{u}_k) \leq 0 \qquad k = 1, ..., K \tag{6.5}$$

with $\mathbf{x}$ the system variables that are the same in pre- and post-contingency state (i.e., the control variables) and $\mathbf{u}_k$ the system variables that can be changed following a contingency k (i.e., the state variables). The index 0 refers to the pre-contingency state. K different contingencies are considered.

Equation 6.1 gives the objective function, i.e., minimization of the operational system cost in the pre-contingency state. Equations 6.2 and 6.3 represent the technical constraints of the power plants (generation limits, ramping limits, minimum up and down time), the market clearing condition and the technical constraints of the electricity grid (power flow equations, transmission limits) in the pre-contingency state. Equations 6.4 and 6.5 represent the same set of constraints in the different post-contingency states. The grid constraints can be the AC power flow equations or the DC power flow equations.

In a unit commitment model with DC power flow, subject to the N-1 security criterion, the following system variables play a role:

- The unit commitment decision (i.e., on/off state of each power plant) is a control variable. Switching a power plant on or off takes too long, making it unsuitable to deal with contingencies.
- The economic dispatch decision (i.e., generation dispatch, pump usage and renewables curtailment) can be a control variable or a state variable. In the preventive approach, the economic dispatch decision are control variables. In the corrective approach, the economic dispatch decision are state variables.
- The grid operation decision (i.e., phase shifter angels and HVDC flows) can be a control variable or a state variable. In the preventive approach, the grid operation are control variables. In the corrective approach, the grid operation are state variables.

6.2 Determining a N-1 secure system operation

Determining the optimal N-1 secure operation of a power system can be computationally challenging. Two important parameters that influence the solution time of the optimization model are (1) the number of post-contingency actions and (2) the number of considered contingencies.

The number of possible post-contingency actions depends on the approach taken. The preventive approach does not allow post-contingency actions, whereas the corrective approach allows a change in the economic dispatch and the setting of flexible grid elements.

The number of possible contingencies increases with the size of the electricity grid. In a grid with L lines, L+1 system states should be considered (one pre-contingency state and L post-contingency states). For a grid of realistic size, the number of possible contingencies might become large. Different ways exist to deal with the large number of possible contingencies.

- Full optimization. The optimal N-1 secure operation of the power system is found if all possible contingencies are taken into account in the optimization. However, this approach can not be used for a large-scale electricity grid as the optimization model will become too large to solve.

- Iterative approach. The optimal N-1 secure operation can be determined by adding iteratively contingencies to the optimization model. In a first iteration, the model determines the optimal system operation in the post-contingency state. The line outages for which this solution is not N-1 secure are added to the optimization model, after which a new optimization takes place. This iterative process continues until a N-1 secure solution is found. The disadvantage of this approach is that the optimality of the found solution is not guaranteed.
- Umbrella approach. In the umbrella approach, the critical contingencies are determined ex-ante and taken into account in the optimization. The set of critical line outages is defined as the set of minimum size that is required to describe the feasible solutions of the optimization [16].
- TSO expertise. The transmission system operator (TSO) might be able to define the critical contingencies ex-ante based on its knowledge of the power system. Taking these critical contingencies into account in the optimization should lead to a N-1 secure operation of the power system.

Chapter 7

Integration of DC power flow in unit commitment

A first section of this chapter describes how the DC power flow model is implemented in a unit commitment model. In a second section, some relevant economic grid parameters are discussed and in a third section is the DC power flow validated.

7.1 Implementation in unit commitment

The objective function of a unit commitment model is to minimize the overall operational system cost. This includes transmission costs. The objective function becomes

$$min \left(\sum_{T} \sum_{I} \left(c_{I,T}^{prod} + c_{I,T}^{start} + c_{I,T}^{stop} \right) + \sum_{T} \sum_{L} c_{L,T}^{trans} \right) \tag{7.1}$$

with T the set of time steps, I the set of power plants, L the set of transmission lines (AC and DC), $c_{I,T}^{prod}$ the production cost, $c_{I,T}^{start}$ and $c_{I,T}^{stop}$ respectively the starting and stopping cost and $c_{L,T}^{trans}$ the transmission cost. All cost parameters are expressed in [EUR/timestep].

The transmission cost $c_{L,T}^{trans}$ of a line L at time step T follows from

$$max \left(-P_{L,T} \cdot TC_L \, , \, P_{L,T} \cdot TC_L \right) = c_{L,T}^{trans} \qquad \forall L, T \tag{7.2}$$

with the transmission cost per unit TC_L in [timestep $\cdot$ EUR/MWh] and the power flow $P_{L,T}$ in [MW]. A transmission tariff can reflect technical aspects (e.g., losses) or economic aspects (e.g., congestion rents).

The market clearing condition must hold for every node or zone in the grid.

$$G_{N,T} = D_{N,T} + P_{N,T} \qquad \forall N, T \tag{7.3}$$

with $G_{N,T}$ the total generation in [MW], $D_{N,T}$ the total load in [MW] and $P_{N,T}$ the power injection in the grid in [MW]. The power injection in the grid can be positive (generation exceeds load) or negative (load exceeds generation).

The grid constraints consist of equality constraints linking grid injections with grid flows and inequality constraints limiting the line flows and phase shifter angles. The DC power flow relation between grid injections and line flows, in its most extended form, is

$$\mathbf{p}_{L_{AC},T} = \sum_{Y} \mathbf{PTDF}_{Y} \cdot \mathbf{p}_{Y,N,T} + \mathbf{PSDF} \cdot \boldsymbol{\alpha}_{L_{AC},T} + \mathbf{DCDF} \cdot \mathbf{p}_{L_{DC},T} + \mathbf{p}_{L}^{0} \quad \forall T \tag{7.4}$$

In nodal grid models, the *zero imbalance* flow is zero and the set Y can be dropped as it is not relevant to work with injections per type. In case of injections per type, each injection type is limited to the generation or load of that type (see equation 5.7) and the net injection is the sum of the injections per type (see equation 5.8). The PSDF-matrix only exists in a grid with phase shifting transformers and the DCDF-matrix is only useful for a grid with DC lines.

The line flows are limited by the line capacities, both for AC lines and DC lines.

$$\mathbf{p}_{L,min} \leq \mathbf{p}_{L,T} \leq \mathbf{p}_{L,max} \tag{7.5}$$

The phase shifter angle is constrained to the operation range of the phase shifting transformer.

$$\boldsymbol{\alpha}_{L,min} \leq \boldsymbol{\alpha}_{L,T} \leq \boldsymbol{\alpha}_{L,max} \tag{7.6}$$

In a realistic unit commitment simulation, certain simplifications have to be made about the boundaries of the considered power system. The neglected neighbouring power systems can be included in the simulation in different ways. The historical or expected import/export at the boundary of the considered power system can be included in the residual electricity demand of the considered power system. Another approach is to represent the power system outside the considered area by a dummy node with a certain load profile and generation profile.

An extended model description of the unit commitment model, formulated as a mixed-integer linear program, can be found in [17].

7.2 Economic grid parameters

An important aspect of the market design is the pricing mechanism. In a nodal pricing market, all grid constraints are taken into account during the market clearing and the electricity price is determined as the shadow price of the market clearing condition (i.e., the marginal price). This might result in a different electricity price at every node. A nodal pricing system is based on a nodal grid model. Nodal pricing is also often referred to as locational marginal pricing. In a zonal pricing market, only one electricity price per zone exists. This implies that intra-zonal congestion is neglected. A zonal pricing system is based on a zonal grid model in which the zonal electricity price is determined as the shadow price of the market clearing condition (i.e., the marginal price). However, due to the simplified zonal grid model, a zonal market clearing might give an infeasible system solution. Therefore, a redispatch after the market clearing might be required in a zonal pricing market. Nodal pricing gives a more correct price signal to the market participants, in accordance with the grid constraints [18].

An important economic parameter in congested electricity grids is congestion rent. Congestion rent (or congestion revenue) is a line parameter defined as the price difference between the end nodes of the line times the flow through the line [19]. The congestion rent is an indicator for the economic value of a transmission line and serves as the basis for transmission right price determination. A transmission right is a right to use the transmission grid to transmit a certain power during a certain time slot [20]. Congestion rents can also be used as the basis of a grid investment analysis.

7.3 Validation of the DC power flow in unit commitment

This section describes a case study of the DC power flow, implemented in an unit commitment model as described in this text, in order to validate the model. The simulation results following from the unit commitment model with DC power flow are compared with the optimal power flow results following from MATPOWER [21].

Consider a simple network with 3 nodes and 3 lines (see figure 7.1). All lines have equal line impedances. A 1000 MW power plant is connected to node 1 with a marginal generation cost of 10 EUR/MWh. A 500 MW power plant is connected to node 2 with a marginal generation cost of 20 EUR/MWh. A load is connected to node 3, varying from 0 to 1500 MW. As the focus is on validating the grid model, the dynamic constraints of the power plants are neglected.

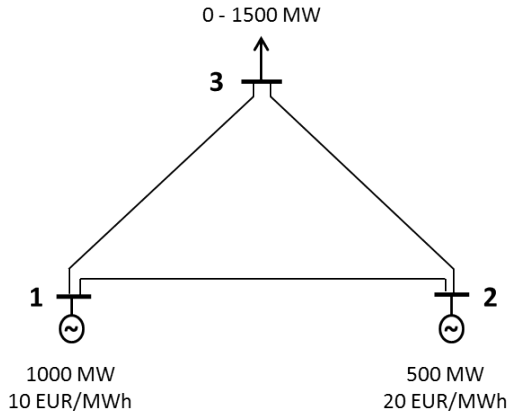

Figure 7.1: Simple 3-node network, used to validate the DC power flow.

In case of unlimited transmission capacity between the nodes, the power plant at node 1 would deliver all required power up to a level equal to its installed capacity, as of where the power plant at node 2 starts generating (see figure 7.2). Up to a load of 1000 MW, the flow through line 1-3 is twice the flow through lines 1-2 and 2-3. For higher loads, power is injected in the grid at node 2, causing a decrease in line flow 1-2 and an increase in line flow 2-3. No loss of load occurs and the total system cost, aggregated over all load levels, is 135 kEUR. The simulation results from the UC model match the simulation results from MATPOWER for this case.

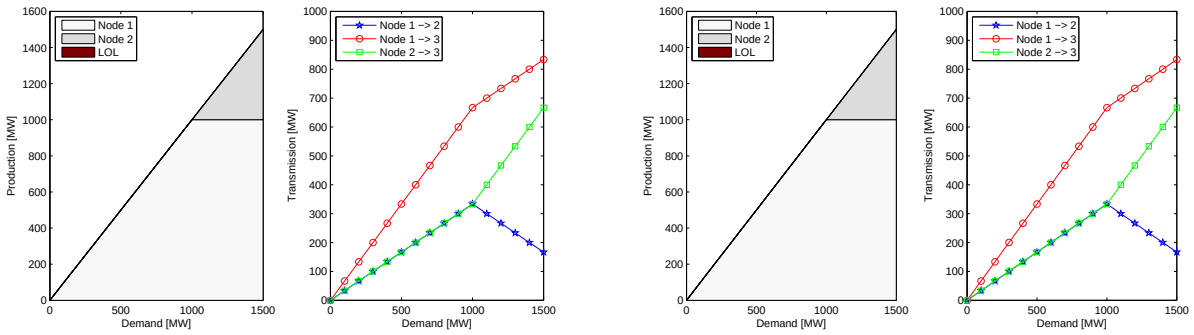

(a) UC with DC power flow

(b) OPF Matpower

Figure 7.2: Generation and flows for the simple 3-node network as function of the demand at node 3, in case of unlimited transmission capacity. LOL refers to loss of load.

In a more realistic scenario with limited transmission capacity, the picture looks different. Assume a transmission capacity of 750 MW for each line. Figure 7.3 gives the generation and flows in this situation. It becomes clear that the more expensive power plant at node 2 is more often used than in the previous situation and that load shedding occurs. Although transmission lines 13 and 23 have together a capacity of 1500 MW, the physical characteristics of the network (impedances) do not allow to use both transmission lines at full capacity at the same time. The grid constraints cause an increase in total system cost from 135 kEUR to 585 kEUR (with 3000 EUR/MWh cost of lost load). The simulation results from the unit commitment model match the simulation results from MATPOWER.

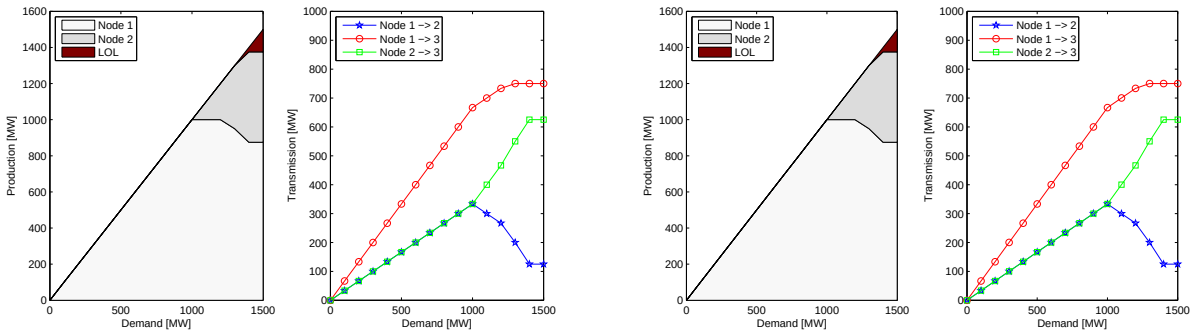

(a) UC with DC power flow

(b) OPF Matpower

Figure 7.3: Generation and flows for the simple 3-node network as function of the demand at node 3, in case 750 MW transmission capacity for each line. LOL refers to loss of load.

Power flow devices like phase shifting transformers (PST) and high voltage DC lines (HVDC) bring extra flexibility in the grid. Figure 7.4 and figure 7.5 show the generation and flows in the 3-node network with respectively a PST at line 13 and a HVDC link replacing line 13 (with the same transmission capacity). A PST reduces some of the lost load and with HVDC line no loss of load occurs. The simulated generation from the unit commitment model match the simulation results from MATPOWER. A PST enables to increase or decrease the power flow through the line were its located. The flow panels of figure 7.4 show that at low load levels, the PST on line 13 attracts extra flow while at higher load levels, flow is shifted to the parallel path (lines 12 and 23). The flow through a HVDC line is fully controllable. Due to this extra degree of freedom, different optimal solutions are possible (see different flows according to the unit commitment simulation and MATPOWER simulation at figure 7.5).

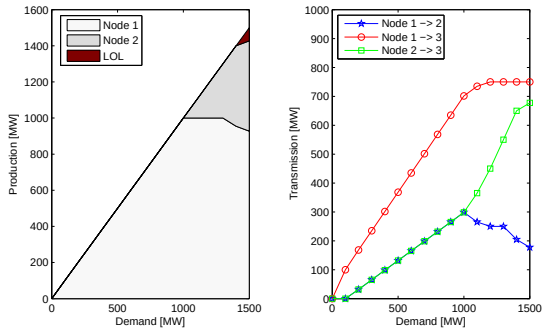

(a) UC with DC power flow

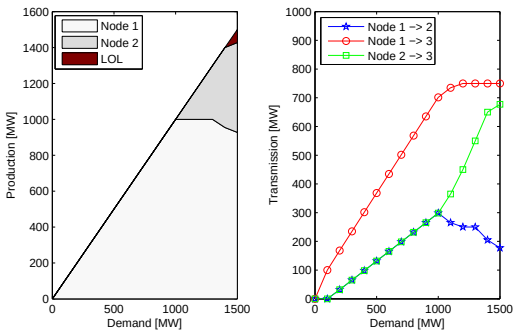

(b) OPF Matpower

Figure 7.4: Generation and flows for the simple 3-node network as function of the demand at node 3, in case 750 MW transmission capacity for each line and a PST on line 13. LOL refers to loss of load.

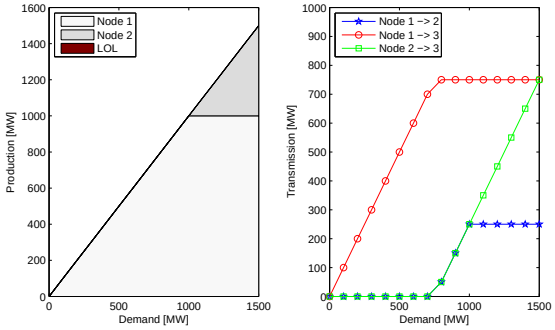

(a) UC with DC power flow

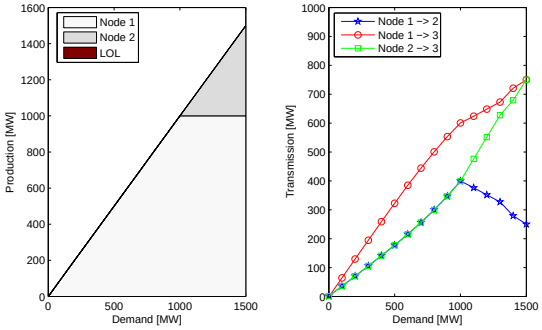

(b) OPF Matpower

Figure 7.5: Generation and flows for the simple 3-node network as function of the demand at node 3, in case 750 MW transmission capacity for each line and a HVDC link between node 1 and 3. LOL refers to loss of load.

Chapter 8

Conclusion

This text presents a comprehensive overview of the DC power flow, consisting of four important parts: the basic DC power flow description (chapter 3), the implementation of power flow controlling devices (chapter 4), the nodal-zonal reduction of grid models (chapter 5) and the implementation of N-1 security (chapter 6).

The DC power flow, as described in this text, is implemented in a unit commitment model (chapter 7). More precisely, the following aspects are implemented:

1. DC power flow including phase shift transformers and HVDC links.
2. The possibility to include zero-imbalance flows and different PTDF-matrices per type.
3. N-1 security optimization, according to the preventive or corrective approach.

This text focuses on the model formulation. Application of the unit commitment model with DC power flow are presented in the following papers:

- Van den Bergh, K., Delarue, E., and D'haeseleer, W. (2014). Improved Zonal Network Models in Generation Scheduling. Submitted to the 18th Power Systems Computation Conference, Wroclaw.
- Van den Bergh, K., and Delarue, E. (2014). Facilitating the Integration of Renewables with Flexible Transmission Systems. Young Energy Economists and Engineers Seminar, Dresden.

Appendices

AC power flow

This section describes the AC power flow, based on Elgerd [1]. The purpose of an AC power flow is to calculate all line flows and nodal voltages, given a certain set of parameters which are known upfront. The unknown parameters or so called state variable, the known parameters are referred to as system variables. The system variables are:

- The admittance matrix $\mathbf{Y}$ of the electricity grid.
- The active power injection P_N and reactive power injection Q_N at PQ-nodes. At these nodes, no generators are located but only loads with known consumption.
- The nodal voltage magnitude $|V_N|$ and active power injection P_N at PV-nodes. These nodes are usually nodes with a generator regulating the voltage and active power.
- The nodal voltage magnitude $|V_N|$ and voltage angle δ_N at the reference node. The voltage angle of this node is set to zero and acts as reference angle for all other nodes. The active power injection at the reference node is free and represents the power losses in the grid. The voltage magnitude at the reference node equals 1 p.u. There is only one reference node in the network.

Each node is characterized by four parameters: active power injection P_N, reactive power injection Q_N, voltage magnitude $|V_N|$ and voltage angle δ_N. Once these parameters are known, the current injections at each node and the current through each line can be easily calculated. The state variables are:

- The voltage magnitude $|V_N|$ and voltage angle δ_N for each PQ-node.
- The reactive power injection Q_N and voltage angle δ_N for each PV-node.
- The active power injection P_N and reactive power injection Q_N at the reference node.

The static power flow equations are derived as follows.

1. The total power injection in the grid at a node can be written as

$$\underline{S}_N = P_N + j \cdot Q_N \tag{8.1}$$

2. The total power injection can also be written as

$$\underline{S}_N = \underline{V}_N \cdot \underline{I}_N^* \quad with \quad \underline{I}_N^* = \sum_Q \underline{y}_{NQ}^* \cdot \underline{V}_Q^* \tag{8.2}$$

The parameter $\underline{y}_{NQ}$ refers to an element in the admittance matrix (see equation 2.8). Equation 8.2 results in

$$\underline{S}_N = |V_N|(\cos\delta_N + j\sin\delta_N) \cdot \sum_Q (G_{NQ} - jB_{NQ})|V_Q|(\cos\delta_Q - j\sin\delta_Q) \tag{8.3}$$

3. Combining equations 8.1 and 8.3 result in

$$\begin{aligned} P_N &= |V_N| \sum_Q \left(G_{NQ}\cos(\delta_N - \delta_Q) + B_{NQ}\sin(\delta_N - \delta_Q)\right)|V_Q| \\ Q_N &= |V_N| \sum_Q \left(G_{NQ}\sin(\delta_N - \delta_Q) - B_{NQ}\cos(\delta_N - \delta_Q)\right)|V_Q| \end{aligned} \tag{8.4}$$

These non-linear equations are referred to as the static power flow equations (SLFE) for an AC power flow.

In an electricity system with N nodes, 4N variables exist (P_N, Q_N, δ_N and $|V_N|$ for each node) and 2N power flow equations can be written down (see equation 8.4). Consequently, 2N variables have to be known upfront to solve the AC power flow.

The system of 2N non-linear static power flow equations for an electricity network with N nodes has to be solved iteratively. In a first step, the initial voltage at each node is often set to 1 p.u. with zero voltage angle (or a solution of a previous solved case is used). In a second step, the active and reactive power injection at each node is calculated with the estimated node voltages by means of equation 8.4. Following from the difference in active and reactive power between two consecutive iterations steps, a new estimation of the voltage magnitudes and voltage angles can be made with the Gauss-Siedel method or the Newton-Raphons method. This iterative process continues until the difference in active and reactive power between two consecutive iterations steps is smaller than the optimality criterion.

The AC power flow as described in this section simulates the operation of the grid. If the purpose of the calculation is to optimize the grid operation (e.g., optimal generation scheduling), one speaks of an optimal power flow analysis.

Transmission losses in the electricity grid

Three different types of losses are encountered in electricity grids. The first type is the resistive losses, caused by line resistances and proportional to the square of the current. The second type is fixed losses, caused by the corona effect in transmission lines (i.e., ionization of the air surrounding transmission lines) and by hysteresis losses and eddy current losses in transformers. These losses can be treated as constant. The third type of losses is called non-technical losses, which is an euphemism for stolen energy from de power system. In Western Europe, 1 to 3 % of the energy is lost in the transmission grid, mainly due to resistive losses [20].

The active power loss caused by line resistivity is expressed as

$$P_{L,loss} = I_L^2 \, R_L \approx (\frac{S_L}{V})^2 \, R_L \approx P_L^2 \, \frac{R_L}{V^2} = P_L^2 \, \tilde{R}_L \tag{8.5}$$

with I_L the current through a line, R_L the resistance of the line, P_L the active power flow through the line, S_L the total power flow through the line, V the line voltage and $\tilde{R}_L$ a kind of adjusted line resistance [22].

In the framework of unit commitment modeling, transmission losses are mostly neglected. Moreover, DC power flow is based on the assumption of lossless lines. Therefore, it is of little relevance to include transmission losses in DC power flow models. However, for the sake of completeness, this appendix proposes a model to incorporate transmission losses in the DC power flow analysis. Implementing equation 8.5 in linear unit commitment models will break the linearity of the model and cause increasing calculation times. Therefore, it is recommended to linearize the quadratic loss equation 8.5 [22].

The transmission losses can be incorporated in the unit commitment model as follows [23]. First, the line losses are allocated to nodes. A simple way of doing this is allocating a line loss evenly over its adjacent nodes.

$$\mathbf{p}_{N,loss} = \frac{1}{2} \, |A^T| \cdot \mathbf{p}_{L,loss} \tag{8.6}$$

Second, the total losses allocated to a node appear as an extra term in the nodal market clearing equation.

$$G_N = D_N + P_N + P_{N,loss} \tag{8.7}$$

Note that only the nodal injection P_N appears in the network equations. The transmission losses allocated to a node $P_{N,loss}$ are not considered in network equations.

Bibliography

[1] O. Elgerd, "Electric Energy Systems Theory: an Introduction", McGraw-Hill, New York, 1971.

[2] K. Purchala, "Modeling and Analysis of Techno-Economic Interactions in Meshed High Voltage Grids Exhibiting Congestion", Ph.D. Thesis, University of Leuven (KU Leuven), December 2005.

[3] R. Baldick, "Variation of Distribution Factors with Loading", IEEE Transactions on Power Systems, vol. 18, no.4, pp. 1316-1323, 2003.

[4] R. Baldick, K. Dixit, and T.J. Oberbye, "Empirical Analysis of the Variation of Distribution Factors with Loading", IEEE Power Engineering Society General Meeting, vol. 1, pp. 221-229, 2005.

[5] K. Purchala, L. Meeus, D. Van Dommelen, and R. Belmans, "Usefulness of DC Power Flow for Active Power Flow Analysis", IEEE Power Engineering Society General Meeting, vol. 1, pp. 454-459, 2005.

[6] D. Van Hertem, "The Use of Power Flow Controlling Devices in the Liberalized Market", Ph.D. Thesis, University of Leuven (KU Leuven), January 2009.

[7] J. Verboomen, "Optimisation of Transmission Systems by use of Phase Shifting Transformers", Ph.D. Thesis, Delft University of Technology (TU Delft), October 2008.

[8] Dirk Van Hertem, Jody Verboomen, Konrad Purchala, Ronnie Belmans, and WL Kling, "Usefulness of dc power flow for active power flow analysis with flow controlling devices", in *AC and DC Power Transmission, 2006. ACDC 2006. The 8th IEE International Conference on*. IET, 2006, pp. 58–62.

[9] A. Ehrenmann and Y. Smeers, "Inefficiencies in European Congestion Management Proposals", Utilities Policy, vol. 13, no.2, pp. 135-152, 2005.

[10] M. Vukasovic and S. Skuletic, "Implementation of Different Methods for PTDF Matrix Calculation in Flow-Based Coordinated Auction", IEEE International Conference on Power Engineering, Energy and Electrical Drives, 2007.

[11] J.B. Bart and M. Andreewsky, "Network Modelling for Congestion Management: Zonal Representation versus Nodal Representation", 15th Power Systems Computation Conference, 2005.

[12] Amprion, Apx-endex, Belpex, Creos, Elia, EnBW, EpexSpot, RTE, and Tennet, "Central Western European Enhanced Flow-Based Market Coupling Feasibility Report", 2011.

[13] CEER - Council of European Energy Regulators, "Security of Electricity Supply", 2004.

[14] Florin Capitanescu, Jose Luis Martinez Ramos, Patrick Panciatici, Daniel Kirschen, Alejandro Marano Marcolini, Ludovic Platbrood, and Louis Wehenkel, "State-of-the-art, challenges, and future trends in security constrained optimal power flow", *Electric Power Systems Research*, vol. 81, no. 8, pp. 1731–1741, 2011.

[15] A Monticelli, MVF Pereira, and S Granville, "Security-constrained optimal power flow with post-contingency corrective rescheduling", *Power Systems, IEEE Transactions on*, vol. 2, no. 1, pp. 175–180, 1987.

[16] Ali Jahanbani Ardakani and François Bouffard, "Identification of umbrella constraints in dc-based security-constrained optimal power flow", 2013.

[17] K. Van den Bergh, K. Bruninx, E. Delarue, and W. D'haeseleer, "A Mixed-Integer Linear Formulation of the Unit Commitment Problem", University of Leuven (KU Leuven) Working Paper, 2013.

[18] W. Hogan, "Transmission Congestion: the Nodal-Zonal Debate Revisited", Harvard University, John F. Kennedy School of Government, Center for Business and Government, 1999.

[19] C. Duthaler and M. Finger, "Evolution of Transmission Rights in the European Electricity Market", Enerday proceedings, Dresden, 2009.

[20] D. Kirschen and G. Strbac, "Fundamentals of Power System Economics", John Wiley and Sons, Ltd, 2004.

[21] R. Zimmerman, C. Murillo-Sánchez, and R. Thomas, "MATPOWER: Steady-State Operations, Planning and Analysis Tools for Power Systems Research and Education", IEEE Transactions on Power Systems, vol. 26, no. 1, pp. 12-19, 2011.

[22] T. dos Santos and A. Diniz, "A Dynamic Piecewise Linear Model for DC Transmission Losses in Optimal Scheduling Problems", IEEE Transactions on Power Systems, vol. 26, no. 2, pp. 508-519, 2011.

[23] F. Schweppe, R. Tabors, M. Caraminis, and R. Bohn, "Spot Pricing of Electricity", Kluwer Academic Publishers, 1988.